Chemical Mechanism of the Gram Stain and Synthesis of a New Electron-Opaque Marker for Electron Microscopy Which Replaces the Iodine Mordant of the Stain

J. A. DAVIES,[1] G. K. ANDERSON,[2] T. J. BEVERIDGE,[3]* AND H. C. CLARK[4]

Department of Chemistry, the University of Toledo, Toledo, Ohio 43606,[1] Department of Chemistry, University of Missouri, St. Louis, Missouri 63121,[2] Department of Microbiology, College of Biological Science,[3] and Department of Chemistry, College of Physical Sciences,[4] University of Guelph, Ontario, Canada N1G 2W1

Crystal violet (hexamethyl-*para*-rosaniline chloride) interacts with aqueous KI-I$_2$ during the Gram stain via a simple metathetical anion exchange to produce a chemical precipitate. There is an apparent 1:1 stoichiometry between anion (I$^-$) and cation (hexamethyl-*para*-rosaniline$^+$) during the reaction and, since the small chloride anion is replaced by the bulkier iodide, the complex formed becomes insoluble in water. It is this same precipitate which forms in the cellular substance of bacteria (both gram-positive and gram-negative types) and which initiates the Gram reaction. Potassium trichloro(η^2-ethylene)-platinum(II), as an electron-opaque marker for electron microscopy, was chemically synthesized, and it produced an anion in aqueous solution which was compatible with crystal violet for the Gram stain. It interacted with crystal violet in a similar manner as iodide to produce an insoluble complex which was chemically and physically analogous to the dye-iodide precipitate. This platinum anion therefore allows the Gram staining mechanism to be followed by electron microscopy.

One of the fundamental principles of diagnostic microbiology is the manner by which bacteria stain during the Gram reaction. Most bacteria respond reliably to the Gram reaction; i.e., some retain the crystal violet-iodide (CV-I) complex (gram-positive), whereas others are decolorized by the ethanol treatment and can be counterstained (gram-negative). This reaction divides the eubacteria into two fundamental groups according to their stainability and is one of the basic foundations on which bacterial identification is built. Yet, after almost 100 years as a diagnostic method, the exact chemical mechanism of the Gram reaction and its effect on cellular structure is imperfectly understood (4). It is the purpose of this paper to outline the chemical nature of the reaction and to design an electron-opaque chemical probe to study the reaction by electron microscopy at the subcellular level. The following paper (Beveridge and Davies [5]) applies this information and technique to *Bacillus subtilis* and *Escherichia coli* to identify the structural and biochemical alterations to these bacteria during the Gram stain.

MATERIALS AND METHODS

The CV-I precipitate. Crystal violet (CV) (0.6199 g, 1.5 mmol) was dissolved in distilled water (50 ml) by using a sonic bath to aid dissolution. Dropwise addition of the iodine-potassium iodide developing solution (1.0 g of iodine + 2.0 g of KI in 300 ml of distilled water) caused immediate formation of a golden-colored precipitate. Addition was continued until precipitation was complete. The precipitate was separated from the fluid by filtration, allowed to air dry, and then held under vacuum at room temperature for 3 h. This procedure gave a yield of 0.2413 g of precipitate. All chemicals were from Fisher Scientific Co.

Chemical synthesis of the potassium TPt electron-opaque probe. Potassium trichloro(η^2-ethylene)platinum(II) (potassium TPt) was prepared from K$_2$(PtCl$_4$) and ethylene, with an anhydrous SnCl$_2$ catalyst as described by Chock et al. (6).

The CV-TPt precipitate. CV (0.6199 g, 1.5 mmol) in distilled water (50 ml) was prepared as above, and a solution of K[PtCl$_3$(C$_2$H$_4$)] (0.5529 g, 1.5 mmol) in distilled water (25 ml) was added dropwise with continued stirring. A green precipitate formed immediately. After 15 min of stirring, the solution was filtered and dried as above. This gave a yield of 0.7413 g of precipitate.

Chemical and physical examinations. CV (alone), CV-I, and CV-TPt were each examined by conductivity measurements, IR, UV, and visible spectroscopy, and proton nuclear magnetic resonance analyses (^{1}H-NMR).

Conductivity measurements were made for 10^{-3} M acetonitrile solutions by using a Wayne Kerr universal bridge operating at 1,592 Hz ± 1%, equipped with an Ostwald conductivity cell containing platinized electrodes. Solutions were equilibrated to 25.0 ± 0.1°C for
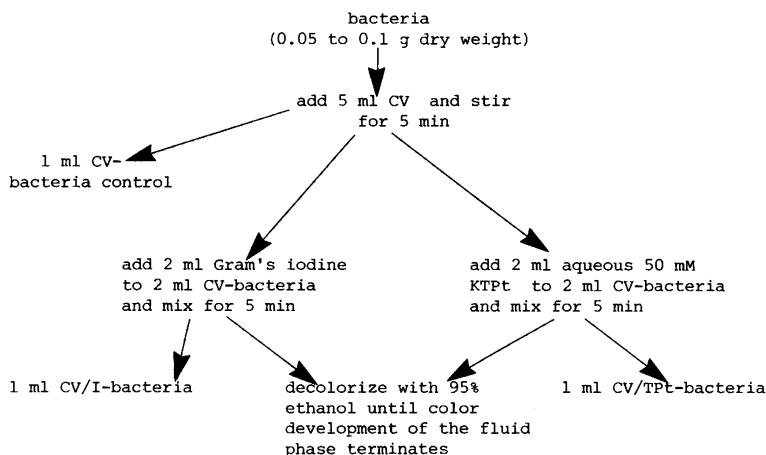
bacteria
(0.05 to 0.1 g dry weight)

add 5 ml CV and stir
for 5 min

1 ml CV-
bacteria control

add 2 ml Gram's iodine
to 2 ml CV-bacteria
and mix for 5 min

add 2 ml aqueous 50 mM
KTPt to 2 ml CV-bacteria
and mix for 5 min

1 ml CV/I-bacteria

decolorize with 95%
ethanol until color
development of the fluid
phase terminates

1 ml CV/TPt-bacteria

FIG. 1. Gram staining regimen used in this study. Bacteria used were either *B. subtilis* 168 or *E. coli* K-12 AB264. CV, Crystal violet as the chloride salt; Gram's iodine, an aqueous solution of iodine and potassium iodide; KTPt, potassium TPt. Typically, after four to five 25-ml ethanol washes, the fluid phase in matched quartz cuvettes approached an absorbance at 660 nm of 0.05, by using a 1-cm path length in a Unicam SP500 series 2 spectrophotometer.

15 min in a water bath equipped with an Omega 4200 control unit. IR spectra were obtained over the range 4,000 to 625 cm^{-1} as nujol mulls by using NaCl optics on a Perkin Elmer 621 spectrometer. UV and visible spectra were obtained over the range 880 to 220 nm as acetonitrile solutions by using matched Infrasil cells of 1-cm path length on a Beckman DU8 spectrometer. ^{1}H-NMR spectra were obtained as D$_2$O or acetone-d^6 solutions in 5-mm tubes at ambient temperature with a Joel FX90Q spectrometer operating in the Fourier transformation mode at 90 MHz. Chemical shifts were given relative to external tetramethylsilane by using the convention that more positive spectral shifts represent deshielding.

Electron microscopy and EDS. Bacteria were grown to an exponential growth phase (for *Bacillus subtilis*, the optical density at 600 nm was 0.60; for *Escherichia coli*, the optical density at 600 nm was 0.63) in 200 ml of nutrient broth or LB broth (3; both broths, Difco Laboratories). The cells were harvested by centrifugation (4,000 × *g*) and washed twice in 50 ml 0.05 M HEPES (*N*-2-hydroxyethylpiperazine-*N'*-2-ethanesulfonic acid) (pH 6.8) containing 1 mM MgCl$_2$. They were then processed according to the Gram regimen as outlined in Fig. 1. After this process, the cells were equilibrated back to 0.05 M HEPES (pH 6.8)–1 mM MgCl$_2$ and fixed for 1 h in 5% (vol/vol) glutaraldehyde in buffer. They were next washed three times in buffer and processed into Durcupan (Fluka AG, Buchs SF, Switzerland), a water-miscible plastic, to circumvent dehydration effects on the CV-I or CV-TPt complexes. This plastic appeared to increase the Pt detection signal (in energy dispersive X-ray analysis [EDS]) twofold over more conventional Epon 812 embeddings. Although iodine has the ability to scatter electrons (Z$_I$ = 53), it is highly volatile under the electron beam. Platinum (Z$_{Pt}$ = 78), and hence TPt, is much more stable and has proven to be an easily monitored probe.

Electron microscopy was performed on a Philips EM400T equipped with a scanning transmission electron microscope (STEM) module, a cryotransfer unit, a low-electron-dose module, and an EDAX 9100/40 energy dispersive system. Point EDS analyses were performed at 20 kV by using a spot size of 20.0 nm; counting times were typically 300 s (live time). Elemental distribution maps were generated by interfacing the EDS system with the STEM module, and the cells were scanned with a 10.0-nm beam. In an effort to preserve the iodine signal in the CV-I material, specimen temperatures of −100 to −196°C were used.

Atomic absorption spectroscopy. Material containing the platinum probe was hydrolyzed in fuming HNO$_3$ containing 250 μg of CsCl per ml to counteract ionization effects and analyzed with a Perkin-Elmer model 2380 atomic absorption spectrophotometer working in the C$_2$H$_4$-N$_2$O flame mode.

RESULTS AND DISCUSSION

Mechanism of the Gram stain. Since the early 1900's, there have been a number of attempts to elucidate the mechanism of the Gram staining response. There are, of course, two separate camps (1): those who suspect a specific cellular substance to be responsible (Table 2 is representative), and those who feel that a permeability difference exists between cell types. Today, most believe that it is a fundamental difference between the molecular architectures of the envelopes of gram-positive and -negative cells which determines the staining response (4). Certainly gram-positive bacteria relinquish their capacity to retain the CV-I complex when their envelope is perturbed by mechanical crushing (2) or by lysozyme digestion (23, 26). These same cells stain gram-negative after protoplast formation (11). Salton has clearly demonstrated that more
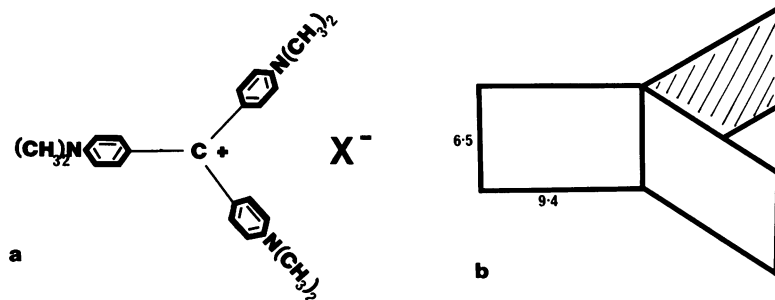
FIG. 2. (a) Model of the CV molecule. (b) Dimensional and shape aspects of the molecule. The measurements are in angstroms.

cellular ^{32}P was released from gram-negative than from gram-positive cells during the decolorization (ethanol) step (22). Unwittingly, Christian Gram has provided us with a clue to cell wall structure and chemistry (12).

CV (hexamethyl-*para*-rosaniline chloride) is a stable carbocation dye of the structure seen in Fig. 2a, where X = Cl. The ^{1}H-NMR spectrum of this compound confirms this structure. Unlike the structure Gurr has proposed in *Encyclopedia of Microscopic Stains* (13), which is only a minor resonance form of the carbocation, there are (in real time) no double bonds available for chemical substitution in this molecule.

A D$_2$O solution of CV gives rise to a singlet resonance at 3.00 ppm of integrated intensity 3.0, owing to the equivalent *N*-methyl protons and an AB pattern centered at 7.11 ppm of integrated intensity 2.3, owing to the protons of the 1,4-disubstituted aromatic rings. The IR spectrum exhibits absorptions as expected for a 1,4-disubstituted aromatic structure (1,581, 1,227, 1,162, 1,061, 832, and 806 cm^{-1}). Weak bands at 1,302 and 1,191 cm^{-1} may be attributable to the presence of C–N bonds. Conductivity

measurements of a 10^{-3} M solution of CV in acetonitrile yielded a value for the equivalent conductivity (Λ_E) of 176.1 ohm^{-1} cm^2 mol^{-1}. This value is typical of 1:1 electrolytes with reported values ranging from 92 to 199 ohm^{-1} cm^2 mol^{-1}, and values of ca. 160 ohm^{-1} cm^2 mol^{-1} have been typically observed (10). The electronic spectrum in acetonitrile solution showed the absorptions characteristic of this type of chromophore (λ_{max} = 580, 510 [sh.], 445, 400, 310, and 250 nm).

A comparison of the above data with those for the CV-I and CV-TPt complexes is shown in Table 1. More detailed information is available in the Appendix. It is apparent from these results that there is a close resemblance between all three chemical forms and that CV-I and CV-TPt are chemically and physically analogous structures. They are, therefore, directly comparable to one another.

Furthermore, CV reacts with the iodide (either I$^-$ or I$_3^-$ are possible) anion of Gram's iodine (a solution of iodine and potassium iodide) via a metathetical anion exchange. This replaces the small chloride anion of the original

TABLE 1. Comparison of CV and its CV-I and CV-TPt complexes

Criterion	Characteristic of:		
	CV	CV-I	CV-TPt
Λ_E (ohm^{-1} cm^2 mol^{-1})	176.1	181.6	174.3
IR (cm^{-1})	1,581, 1,227, 1,162, 1,061, 832, and 806	Identical	Identical
λ_{max} (nm)	580, 510 (sh.), 445, 400, 310, and 250	585, 505 (sh.), 375, 355, 300, and 250	590, 510 (sh.), 375, 350, 295, and 250
^{1}H-NMR	Equivalent *N*-methyl protons	Too insoluble in D$_2$O or acetone-d^6 for H-NMR study	Equivalent *N*-methyl protons
	Equivalent 1,4-disubstituted aromatic rings		Equivalent 1,4-disubstituted aromatic rings
Reaction		1 cation to 1 anion	1 cation to 1 anion

TABLE 2. Specific substances to which the Gram response has been attributed

Substance	Researcher (yr)
Lipoproteins	Stearn and Stearn (1924, 1930)
Lipids	Eisenberg (1910); Schumacher (1928)
Nucleic acids and nucleoproteins	Deussen (1921), Dubos and MacLeod (1938), Henry, Stacey and Teece (1945), Henry and Stacey (1946), Webb (1948)
Carbohydrates	Webb (1948)
Glycerophosphates	Schumacher (1928), Mitchell and Moyle (1950, 1951, 1954)
Polyamines	Herbst, Weaver, and Keister (1958)
Mg-ribonucleates	Henry, Stacey, and Teece (1945)
Glycerol and ribitol phosphate esters	Mitchell and Moyle (1958)

CV salt with the bulkier I^- or I_3^- anions to form a chemical complex which precipitates from aqueous solution. Unlike the dye-to-iodine ratio of 1:2 reported by Wensinck and Boeve (29), there is an apparent 1:1 stoichiometry between anions and cations, according to conductivity measurements (Table 2). This exact same mechanism is at work when the iodide of the Gram reaction is replaced by the bulky TPt anion. Accordingly, this electron-dense, platinum probe can be used without disturbing or altering the mechanism of the Gram stain; i.e., *B. subtilis* stains gram positive (Fig. 3), unless the cell wall is perturbed (Fig. 4 shows lysozyme digestion), and *E. coli* stains gram negative (Fig. 5).

This information suggests that the Gram stain depends on the simple chemical mechanism of metathetical anion exchange. CV is a water-soluble molecule which dissociates into CV^+ and Cl^- on dissolution; the carbocation is shaped like a three-bladed propeller. Each of the three N-methylated, aromatic rings in its structure forms a blade of the propeller, is ca. 0.94 nm long and 0.65 nm thick, and joins at a central carbon (Fig. 2b). This cation (and presumably the 0.362-nm diameter Cl^-) is able to penetrate through the enveloping layers of both gram-positive and -negative bacteria to the cytoplasmic substance. (Holes ca. 1.88 nm in diameter must exist.) When Gram's iodine is added, I^- or I_3^- (diameter, 0.432 or 0.607 nm) encounters and interacts with CV^+ to form a CV-I precipitate. This happens, presumably, both within (21, 25) and without the cell. The addition of ethanol (as a decolorizing fluid) washes away the precipitate from around and outside the cell. CV-I is too large to escape from the cytoplasmic substance unless the enveloping layers of the bacterium are perturbed (Fig. 3 and 4; and see accompanying paper [5] for further details). It seems unlikely that the CV^+ interaction with constituent cellular anions contributes to the Gram stain since

the addition of iodide (or TPt) is necessary to give an unequivocal staining response (23).

Use of TPt as an electron-opaque marker for electron microscopy to study the Gram stain. To study the cellular response accurately during the Gram stain, we felt it necessary to design and use a probe suitable for electron microscopy which would identify the dye substance. In this way, the dye could be followed through cellular space, and its eventual location could be determined. In addition, electron microscopy would allow the elucidation of cellular damage during the staining regimen.

Initially, we believed that it was feasible to incorporate a heavy metal directly into the CV molecule since the available information suggested that reactive chemical sites existed within its structure (13). Our own data suggest the structural form seen in Fig. 2a and all our attempts to label this molecule failed. Next, we felt that it may be possible to follow the iodide during the staining reaction since its mass ($Z_I = 53$) is suitable for electron microscopy. In our hands, this anion proved too volatile, even at very low specimen temperatures (down to $-196°C$), to be preserved under the electron beam (Fig. 6a, b, and c).

Our expertise with organic platinum compounds led us to identify TPt as a possible candidate to probe the Gram reaction; it was chemically synthesized and used to replace iodide during the staining reaction. All our data (Table 2, Fig. 3 to 5) indicated that this anion was suitable for the Gram stain. The TPt anion is even larger than the I^- (an elipsoid, 0.823 by 0.615 nm); it efficiently precipitated the CV^+. Unstained thin sections of bacteria (both *E. coli* and *B. subtilis*) treated sequentially with CV^+ and TPt^- to form CV-TPt revealed electron-opaque areas within the cells (Fig. 7b and 8a) which produced distinct Pt lines during EDS analysis (Fig. 7d and 8d). In fact, there was
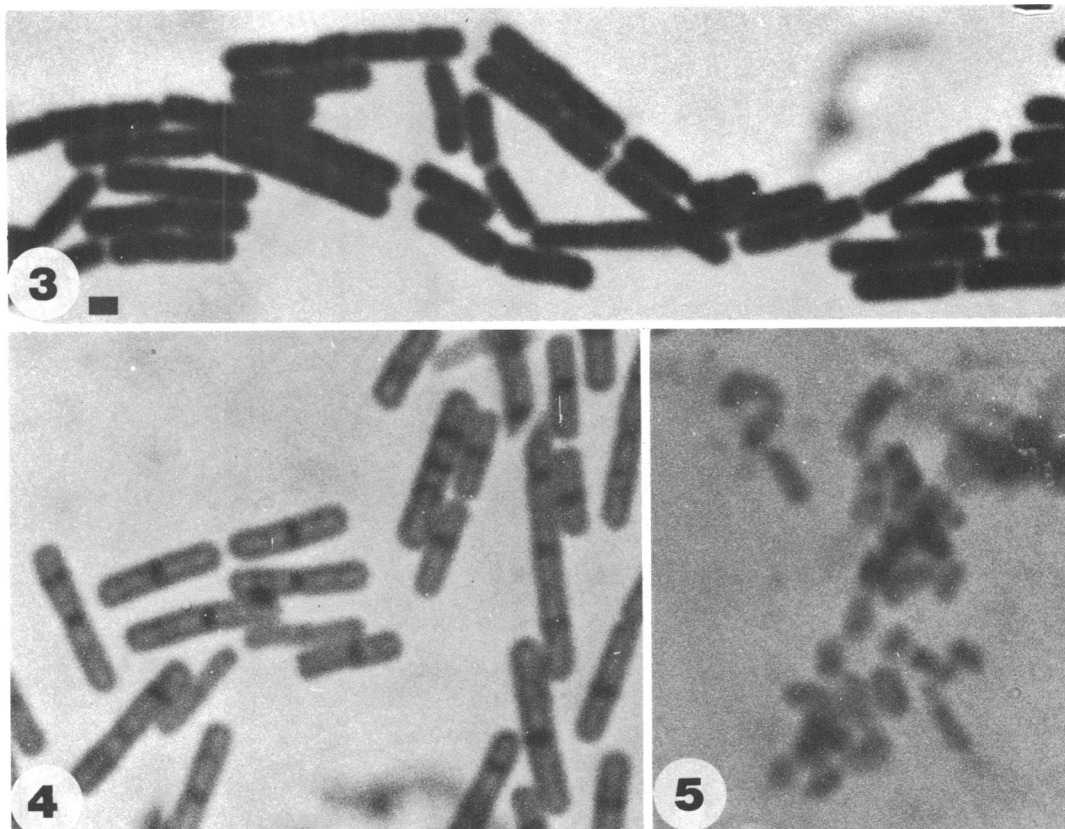
FIG. 3. Light micrograph of gram-positive cells of *B. subtilis*, gram stained with TPt.

FIG. 4. Light micrograph of TPt-stained gram-positive cells of *B. subtilis* which had been treated with 50 µg of lysozyme ml^{-1} for 15 min before staining. They now stain gram-negative since the dye-retaining barrier of the wall has been broken down.

FIG. 5. Light micrograph of TPt-stained *E. coli* staining gram negative (as they should). Figures 3, 4, and 5 are of the same magnification. Bar in Fig. 3 represents 500 nm.

enough TPt in these cells to produce dot maps of its distribution throughout the cell substance of individual bacteria (Fig. 7e and 8e). CV (alone) did not add electron-scattering power to the cells (Fig. 7a). Atomic adsorption analyses revealed that the TPt content of the cells was typically 2.0 to 2.5 nmol mg (dry weight)$^{-1}$. Ethanol treatment severely reduced this TPt concentration in *E. coli* (Fig. 8b), but most of the TPt was retained in cells of *B. subtilis* (Fig. 7b). This electron-dense marker, therefore, seemed suitable for studying the Gram stain mechanism at the ultrastructural level.

APPENDIX

Specific chemical and physical data on the CV-I and CV-TPt precipitates. A comparison of the CV data with that obtained with precipitates formed with KI-I$_2$ and with K[PtCl$_3$(C$_2$H$_4$)] showed that these products

have structures identical to Fig. 2a, except that the anion has been metathetically replaced by I$^-$ (X = I) or by [PtCl$_3$(C$_2$H$_4$)]$^-$ (X = [PtCl$_3$(C$_2$H$_4$)]). These compounds were precipitated from aqueous solution because the small chloride anion was replaced by the bulkier I$^-$ or [PtCl$_3$(C$_2$H$_4$)]$^-$ anions. Both behaved as typical 1:1 electrolytes in acetonitrile solution (Λ_E = 181.6 ohm^{-1} cm^2 mol^{-1} for CV-I and 174.3 ohm^{-1} cm^2 mol^{-1} for CV-TPt). These products appeared to remain ionic after metathesis. Their IR and electronic spectra remained almost identical to CV alone, and there were no IR absorptions due to ν (C=C) modes of the coordinated olefin present in the TPt anion. Such bands are often of low intensity, however, and may be obscured by bands which are due to the CV$^+$ cation (Table 2), since in K[PtCl$_3$(C$_2$H$_4$)] itself, these bands occurred at 1,515 cm^{-1} and 1,243 cm^{-1}, close to the very intense 1,581 cm^{-1} and 1,227 cm^{-1} bands of CV$^+$. However, the presence of coordinated ethylene was confirmed unequivocally by ^{1}H-NMR data (see IR data). The electronic spectroscopic data (λ_{max} = 585,
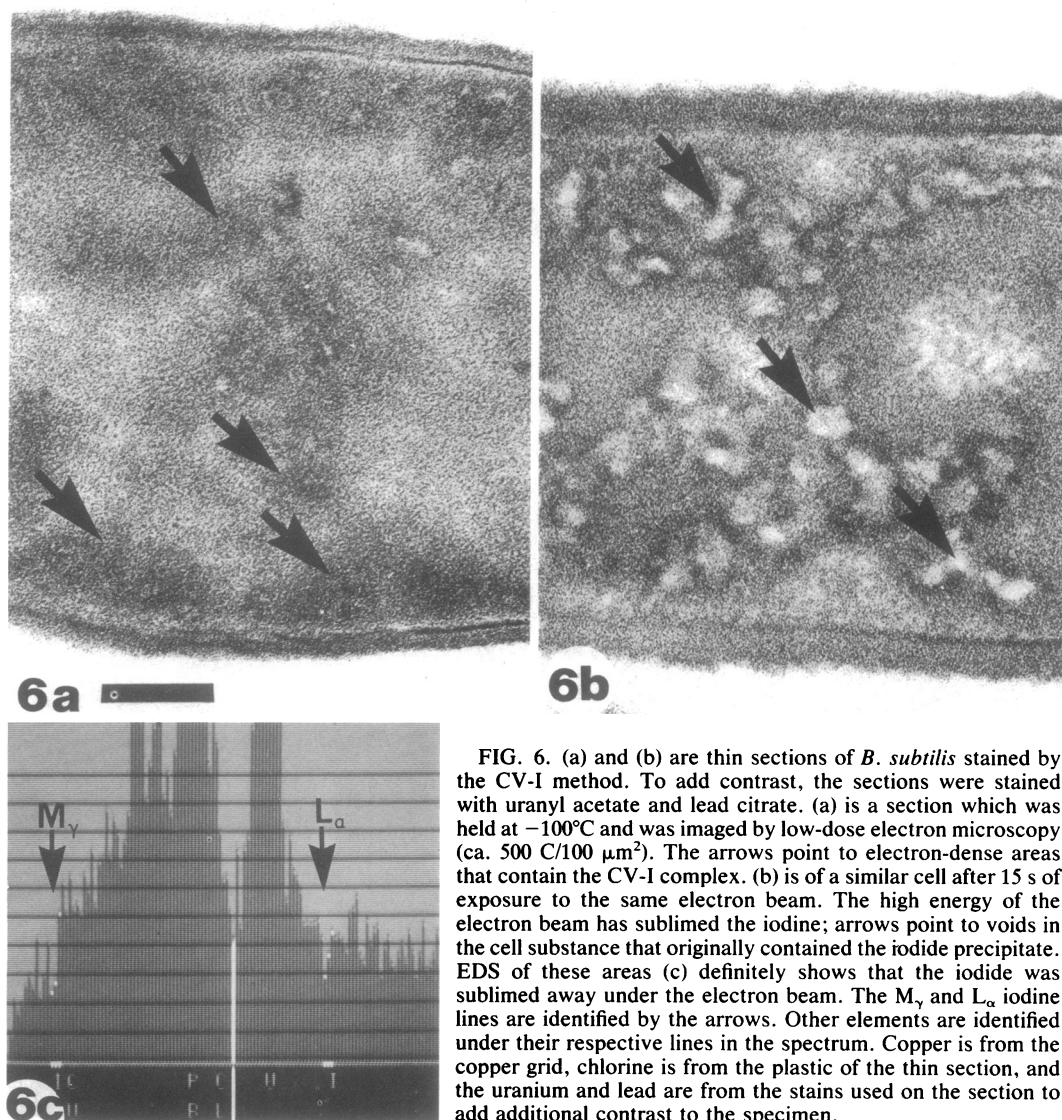
FIG. 6. (a) and (b) are thin sections of *B. subtilis* stained by the CV-I method. To add contrast, the sections were stained with uranyl acetate and lead citrate. (a) is a section which was held at $-100°C$ and was imaged by low-dose electron microscopy (ca. 500 C/100 μm^2). The arrows point to electron-dense areas that contain the CV-I complex. (b) is of a similar cell after 15 s of exposure to the same electron beam. The high energy of the electron beam has sublimed the iodine; arrows point to voids in the cell substance that originally contained the iodide precipitate. EDS of these areas (c) definitely shows that the iodide was sublimed away under the electron beam. The M_γ and L_α iodine lines are identified by the arrows. Other elements are identified under their respective lines in the spectrum. Copper is from the copper grid, chlorine is from the plastic of the thin section, and the uranium and lead are from the stains used on the section to add additional contrast to the specimen.

505 [sh], 375, 355, 300, and 250 nm for CV-I and 590, 510 [sh], 375, 350, 295, and 250 nm for CV-TPt) demonstrated that the chromophore is largely unperturbed by metathesis.

The ^{1}H-NMR spectrum of CV-TPt in acetone-d^6 confirmed the presence of the platinum(II) anion in the metathesis product. Resonances due to the carbocation (δ[phenyl] = 7.23, AB pattern, integrated intensity 2.0; δ[*N*-methyl] = 3.33, singlet, integrated intensity 2.7) were accompanied by a peak at 4.18 ppm, owing to the protons of the coordinated olefin, exhibiting coupling to platinum (^{195}Pt has I = 1/2 and is 33.8% abundant) resulting in a ratio 1:4:1 pattern with ^{2}J (^{195}Pt, ^{1}H) = 63.7 Hz. The integrated intensity of the olefinic proton resonance confirmed the ratio of one cation to one anion. For comparison, the ^{1}H-NMR

spectrum of an acetone-d^6 solution of K[PtCl$_3$(C$_2$H$_4$)] exhibited a resonance at 4.23 ppm with ^{2}J (^{195}Pt, ^{1}H) = 64.2 Hz. Attempts to obtain a satisfactory signal-to-noise ratio in the ^{1}H-NMR spectrum of CV-I with D$_2$O or acetone-d^6 solvents were frustrated by the extremely limited solubility of this metathesis product in these solvents.

Clearly, the IR, visible and ^{1}H-NMR spectroscopic data, in conjunction with the conductivity measurements, confirmed that crystal violet reacts with KI-I$_2$ or K[PtCl$_3$(C$_2$H$_4$)] in aqueous media via a metathetical anion exchange. As such, products obtained by these routes are chemically related, varying only in the anion and possessing identical chromophores, enabling a direct comparison of their staining properties to be made.
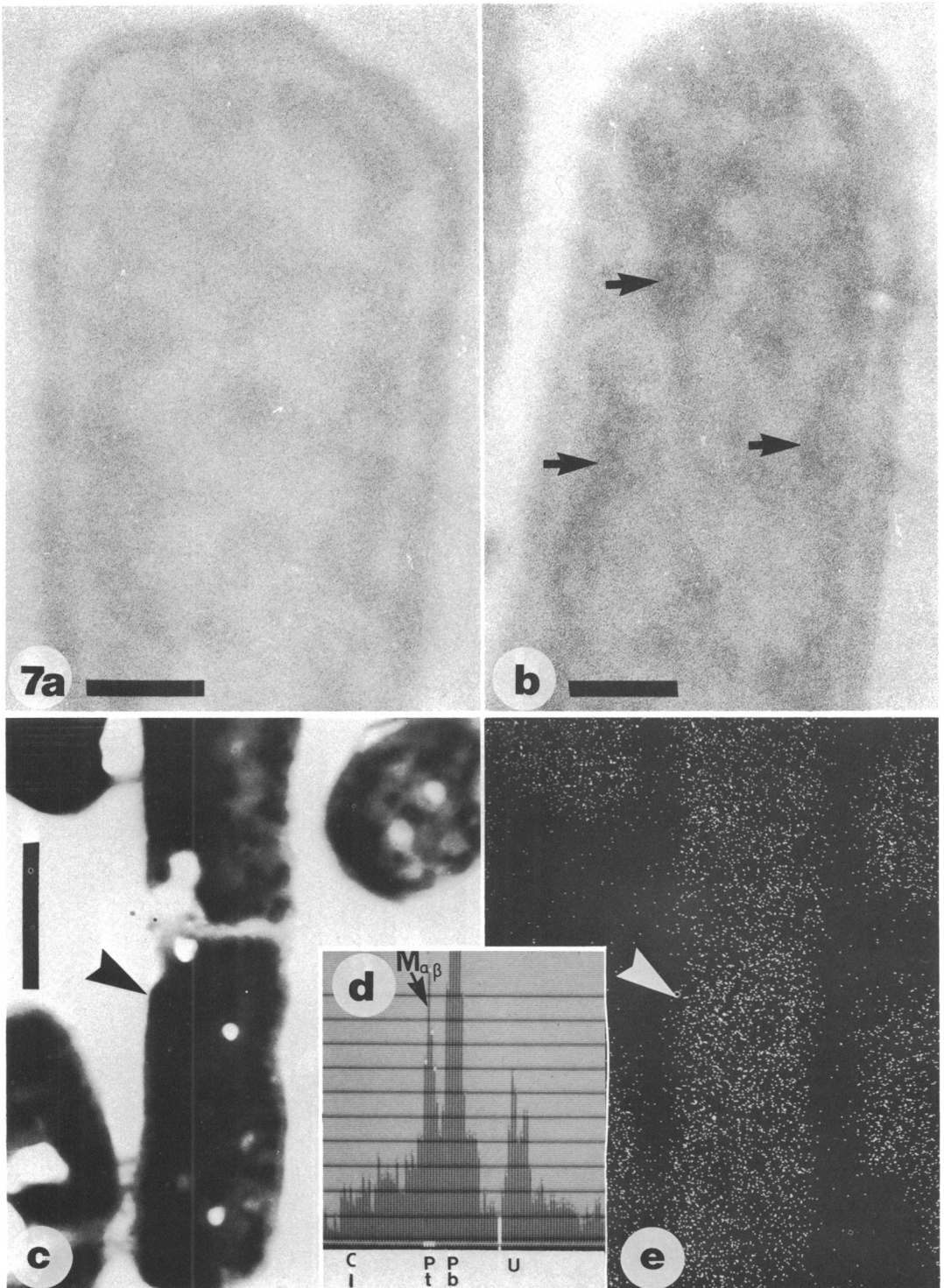
FIG. 7. Thin sections of *B. subtilis* stained by the CV-TPt method. No other contrasting agents have been used. (a) A cell before ethanol treatment and stained with CV only (no platinum); (b) a CV-TPt cell after ethanol treatment. The arrows point to CV-TPt aggregates. Bars in (a) and (b) represent 100 nm. (c) A bright-field STEM image of CV-TPt cells. The contrast has been electronically heightened to emphasize the position of the platinum and these same cells formed the Pt elemental distribution map in (e); bar, 500 nm. (d) An EDS spectrum of an ethanol-treated cell which clearly shows the Pt peak of the TPt. In this instance, uranyl acetate and lead citrate were used to contrast the cell, hence the U and Pb peaks, and the Cu peak is from the copper EM grid and Cl is from the plastic. (e) Is the corresponding elemental distribution map for (c) which shows the Pt (TPt) distribution within the cell. Each dot represents a high concentration of TPt. The arrows in (c) and (e) point to the same area of the cell for easy comparison.
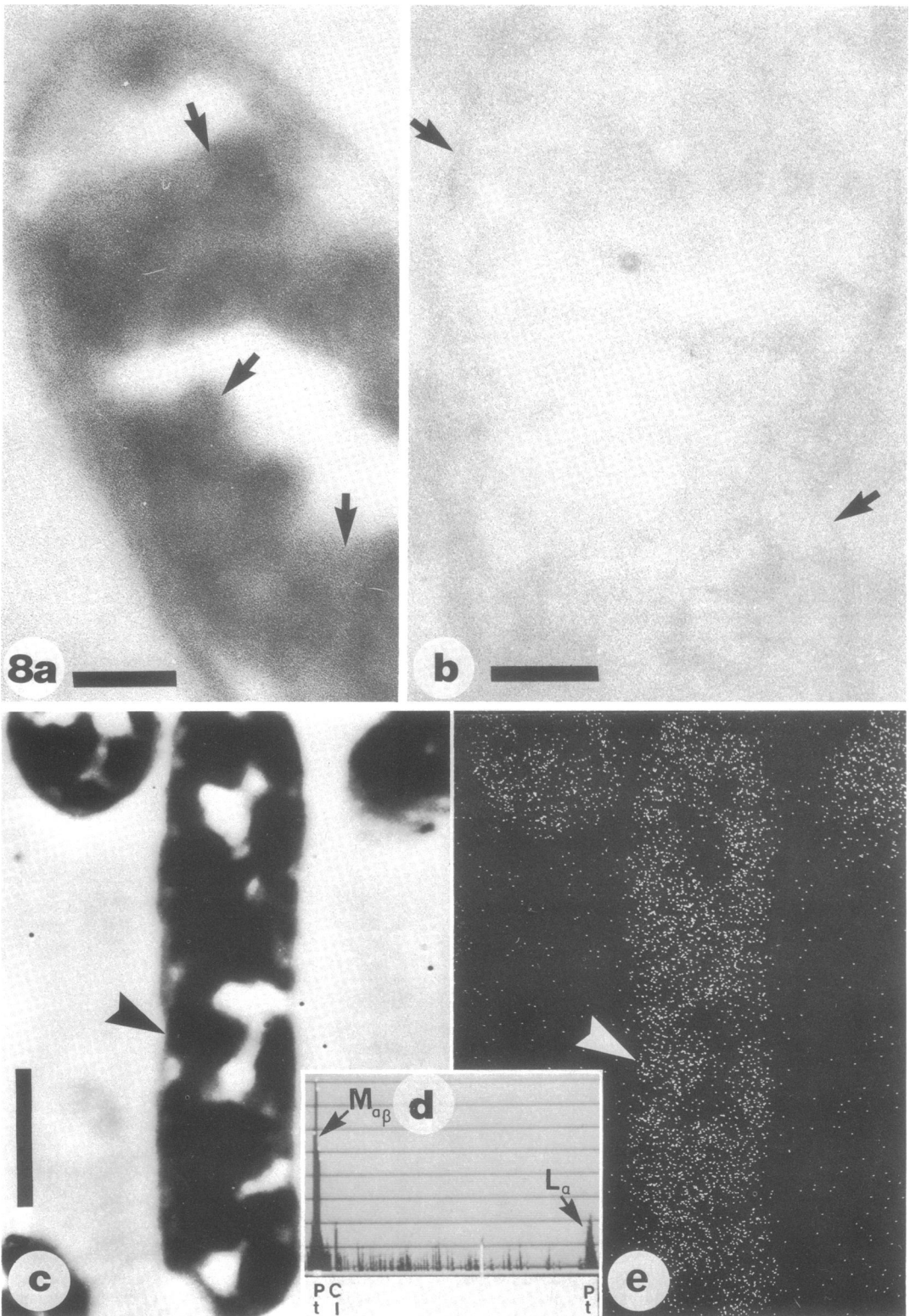
FIG. 8. Thin section of *E. coli* stained by the CV-TPt method. No other contrasting agents have been used. (a) A cell stained with CV-TPt before ethanol decolorization. The arrows point to CV-TPt aggregates. (b) A cell similar to that in (a), but after ethanol treatment. Very little CV-TPt remains to scatter electrons. The arrows point to the cell periphery, and the bars in (a) and (b) represent 100 nm. (c) A bright-field STEM image of a cell before ethanol treatment. The contrast has been electrically heightened, and the bar represents 500 nm. (d) An EDS spectrum of a cell similar to that of (e) which shows the $M_{\alpha,\beta}$ and L_α Pt lines. In this case U and Pb were not used as staining agents, and the small peaks separating the M and L lines are the normal lines present in the background of the continuum. (e) The Pt distribution map of (c). The arrows in (c) and (e) point to the same area of the cell for easy comparison.

LITERATURE CITED

1. **Bartholomew, J. W., and T. Mittwer.** 1952. The Gram stain. Bacteriol. Rev. **16:**1–29.
2. **Benians, T. H. C.** 1920. A further investigation into the principles underlying Gram's stain with special reference to the bacterial cell membrane. J. Pathol. Bacteriol. **23:**401–412.
3. **Bertani, G.** 1951. Studies on lysogenesis. I. The mode of phage liberation by lysogenic *Escherichia coli.* J. Bacteriol. **62:**293–300.
4. **Beveridge, T. J.** 1981. Ultrastructure, chemistry and function of the bacterial wall. Int. Rev. Cytol. **72:**229–317.
5. **Beveridge, T. J., and J. A. Davies.** 1983. Cellular responses of *Bacillus subtilis* and *Escherichia coli* to the Gram stain. J. Bacteriol. **156:**846–858.
6. **Chock, P. B., J. Halpern, and F. E. Paulik.** 1973. Potassium trichloro(ethylene)platinate(II) (Zeise's salt). Inorg. Synth. **14:**90–92.
7. **Deussen, E.** 1921. Die Gramsche Bakterienfarbung, ihr Wesen und ihr Bedeutung. Z. Hyg. Infektionskrankh. **93:**512–522.
8. **Dubos, R. J., and C. M. MacLeod.** 1938. The effect of tissue enzyme upon pneumococci. J. Exp. Med. **67:**791–797.
9. **Eisenberg, P.** 1910. Studien zur Ektoplasmatheorie. IV. Zur Theorie der Gram-festigkeit. Zentralbl. Bakteriol. Parasitenkd. Infektionskr. Hyg. Abt. I Orig. **56:**193–200.
10. **Geary, W. J.** 1971. The use of conductivity measurements in organic solvents for the characterization of coordination compounds. Coord. Chem. Rev. **7:**81–122.
11. **Gerhardt, P., J. W. Vennes, and E. M. Britt.** 1956. Gram reaction of isolated protoplasts and surface membranes of *Bacillus megaterium.* J. Bacteriol. **72:**721.
12. **Gram, C.** 1884. Über die isolirte Färbung der Schizomyceten in Schnitt-und Trockenpräparaten. Fortschr. Med. **2:**185–189.
13. **Gurr, E.** 1960. Encyclopedia of microscopic stains, p. 152–153. Leonard Hill (Books) Ltd., London, England.
14. **Henry, H., and M. Stacey.** 1946. Histochemistry of the Gram staining reaction for microorganisms. Proc. R. Soc. London Ser. B **133:**391–406.
15. **Henry, H., M. Stacey, and E. G. Teece.** 1945. Nature of the Gram positive complex in microorganisms. Nature (London) **156:**720–721.
16. **Herbst, E. J., R. H. Weaver, and D. L. Keister.** 1958. The Gram reaction and cell composition: diamines and polyamines. Arch. Biochem. Biophys. **75:**171–177.
17. **Mitchell, P., and J. Moyle.** 1950. Occurrence of a phosphoric ester in certain bacteria: its relation to Gram staining and penicillin sensitivity. Nature (London) **166:**218–220.
18. **Mitchell, P., and J. Moyle.** 1951. The glycerophospho-protein complex envelope of *Micrococcus pyogenes.* J. Gen. Microbiol. **5:**981–992.
19. **Mitchell, P., and J. Moyle.** 1954. The Gram reaction and cell composition: nucleic acids and other phosphate fractions. J. Gen. Microbiol. **10:**553–540.
20. **Mitchell, P., and J. Moyle.** 1958. The positic acids of *Staphylococcus aureus* and other Gram-positive penicillin-sensitive bacteria: hydrolytic products and possible backbone structure. Proc. R. Phys. Soc. Edinb. **27:**79–90.
21. **Mittwer, T., J. W. Bartholomew, and B. J. Kallman.** 1950. The mechanism of the Gram reaction. II. The function of iodine in the Gram stain. Stain Technol. **25:**169–179.
22. **Salton, M. R. J.** 1963. The relationship between the nature of the cell wall and the Gram stain. J. Gen. Microbiol. **30:**223–235.
23. **Scherrer, R.** 1963. Cell structure and quantitative Gram stain of *Bacillus megaterium.* J. Gen. Microbiol. **31:**135–145.
24. **Schumacher, J.** 1928. Zur Gramschen Farbung. Über die chemische Zusammensetzung der Lipoidsaure und über kunstlich grampositiv gemachte Hefezellen. Zentralbl. Bakteriol. Parasitenkd. Infektionskr. Hyg. Abt. I Orig. **109:**181–192.
25. **Smythe, R. D., and L. Gershenfeld.** 1960. [131]Iodine uptake in the Gram staining technique. Stain Technol. **35:**237–245.
26. **Stearn, E. W., and A. E. Stearn.** 1924. The chemical mechanism of bacterial behavior. II. A new theory of the Gram reaction. J. Bacteriol. **9:**479–489.
27. **Stearn, E. W., and A. E. Stearn.** 1930. Differential action of oxidizing agents on certain gram positive and gram negative organisms. J. Infect. Dis. **46:**500–513.
28. **Webb, M.** 1948. The action of lysozyme on heat killed Gram positive microorganisms. J. Gen. Microbiol. **2:**260–274.
29. **Wensinck, F., and J. J. Boeve.** 1957. Quantitative analysis of the Gram reaction. J. Gen. Microbiol. **17:**401–413.